

# Using Lunar Observations to Assess Terra MODIS Thermal Emissive Bands Calibration

Xiaoxiong (Jack) Xiong

*Earth Sciences Directorate, NASA/GSFC, Greenbelt, MD 20771*

[Xiaoxiong.Xiong-1@nasa.gov](mailto:Xiaoxiong.Xiong-1@nasa.gov)

Hongda Chen

*Sigma Space Corporation, 4801 Forbes Boulevard, Lanham, MD 20706*

## ABSTRACT

MODIS collects data in both the reflected solar and thermal emissive regions using 36 spectral bands. The center wavelengths of these bands cover the 3.7 to 14.24 micron region. In addition to using its on-board calibrators (OBC), which include a full aperture solar diffuser (SD) and a blackbody (BB), lunar observations have been scheduled on a regular basis to support both Terra and Aqua MODIS on-orbit calibration and characterization. This paper provides an overview of MODIS lunar observations and their applications for the reflective solar bands (RSB) and thermal emissive bands (TEB) with an emphasis on potential calibration improvements of MODIS band 21 at 3.96 microns. This spectral band has detectors set with low gains to enable fire detection. Methodologies are proposed and examined on the use of lunar observations for the band 21 calibration. Also presented in this paper are preliminary results derived from Terra MODIS lunar observations and remaining challenging issues.

**Keywords:** Terra, MODIS, calibration, blackbody, Moon

## 1. INTRODUCTION

Since launch in December 1999, more than 10 years of global earth observations have been made by Terra MODIS and used to derive a wide range of data products for studies of changes in the Earth's system of land, oceans, and atmosphere. MODIS is a multispectral filter radiometer and collects data in 36 spectral bands. Twenty of the spectral bands are in the reflected solar region and the other 16 are in the thermal emissive region. The reflective solar bands (RSB), covering wavelengths from 0.41 to 2.2 $\mu\text{m}$ , are calibrated on-orbit using a solar diffuser (SD) and solar diffuser stability monitor (SDSM). The thermal emissive bands (TEB), with wavelengths spanning 3.7 to 14.4 $\mu\text{m}$ , are calibrated by a blackbody (BB). In addition to its on-board calibrators (OBC), MODIS lunar observations, which are scheduled on a near monthly basis, are used to support its on-orbit calibration and characterization<sup>1-3</sup>. Figure 1 shows the MODIS scan cavity and OBC. MODIS also has a space view (SV) port designed for observations to correct instrument background and offset. Regularly scheduled lunar observations are also made through the SV port.

MODIS TEB detectors are calibrated using their responses to the on-board BB on a scan-by-scan (1.4771 sec) basis, with an exception of band 21 at 3.96 $\mu\text{m}$ . This band was designed for fire detection with a specified maximum temperature of 500K. At this temperature, the band 21 spectral radiance is more than 2 orders of magnitude higher than that from the BB nominal operating temperature of 290K for Terra MODIS. The small detector responses, or digital counts, of band 21 to the on-orbit calibration source (BB) coupled with their low signal-to-noise ratios (SNR) are inadequate to derive accurate and stable calibration coefficients for band 21 over its entire dynamic range.

Consequently, band 21 detector calibration coefficients (or gains) are derived using data from periodic BB warm-up and cool-down operations during which the BB temperatures vary from instrument ambient of approximately 272K to 315K. These calibration coefficients are detector and mirror side dependent<sup>4-5</sup>. Figure 2 illustrates Terra MODIS bands 21 (3.96 $\mu\text{m}$ ), 22 (3.96 $\mu\text{m}$ ), 31 (11 $\mu\text{m}$ ), and 32 (12 $\mu\text{m}$ ) middle detector responses in digital numbers ( $dn_{\text{BB}}$ ) as a function of calibration radiances ( $\Delta L_{\text{BB}}$ ) with data from the BB cool-down operation on day 2004115. The calibration radiances  $\Delta L_{\text{BB}}$  have included contributions from the BB, scan mirror, and instrument cavity. The corresponding detector responses  $dn_{\text{BB}}$  are corrected for instrument background provided by the SV observations. Even at 315K, band 21 detector responses are still very small (less than 100 counts) compared to its dynamic range upper limit. Because of this, MODIS band 21 is calibrated using a simple linear algorithm.

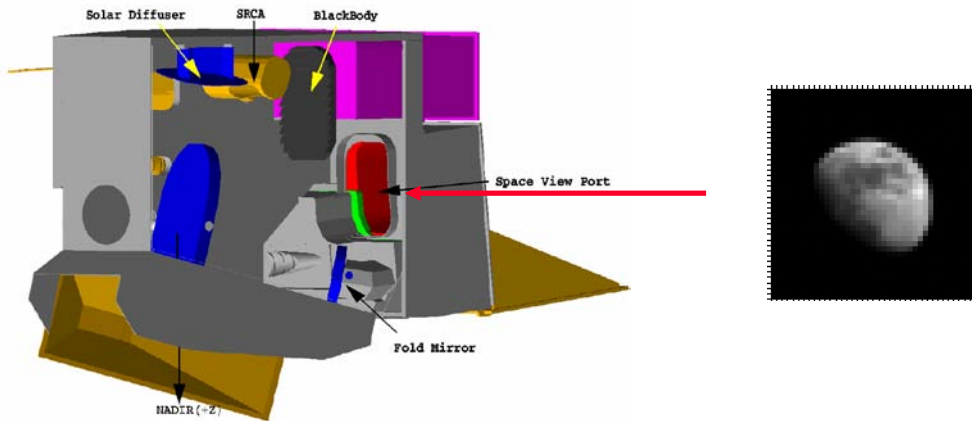


Figure 1: MODIS internal scan cavity, its on-board calibrators (OBC), and lunar observations through the space view (SV) port.

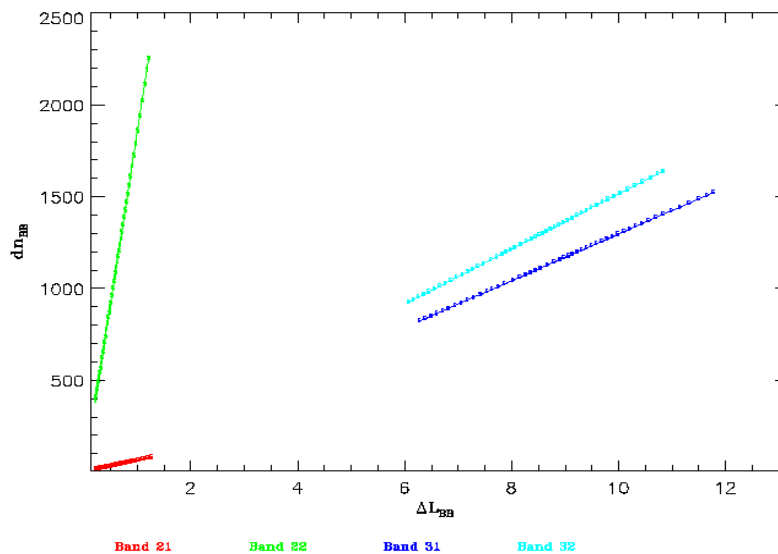


Figure 2: Terra MODIS bands 21, 22, 31, and 32 detector responses in digital numbers ( $dn_{\text{BB}}$ ) as a function of calibration radiances ( $\Delta L_{\text{BB}}$ ). Data from BB cool-down on day 2004115.

Except for band 21, the dynamic ranges of bands 22, 31, and 32 are suitable for deriving high quality calibration coefficients. Based on the design requirements, band 22 has the same relative spectral response (RSR) as band 21 but

with much higher detector gains. As shown in Figure 2, band 22 detector gain is approximately 25 times higher than band 21.

This paper provides an overview of MODIS lunar observations and their applications in support of both the RSB and TEB on-orbit calibration and characterization, including radiometric calibration stability monitoring, spatial characterization, and crosstalk (optical and electronic) assessments. In particular, this paper discusses potential calibration improvements for MODIS band 21 through the use of its lunar observations. Preliminary results derived from Terra MODIS lunar observations are presented. Remaining challenging issues and potential improvements for future studies are also discussed. The approaches developed from MODIS lunar calibration can also be applied to other sensors, such as the NPOESS Preparatory Project (NPP) and Joint Polar Satellite System (JPSS) VIIRS.

## 2. OVERVIEW OF MODIS LUNAR OBSERVATIONS

Since lunar surface reflectance properties are known to be extremely stable, MODIS lunar observations were planned initially to monitor the RSB on-orbit radiometric calibration stability<sup>3</sup>. A special lunar planner tool was developed by the MODIS Characterization Support Team (MCST) in support of its lunar calibration activities. Since launch, lunar observations have been scheduled and implemented on a regular basis for both Terra and Aqua MODIS. Because the lunar surface irradiance strongly depends on the viewing geometry, the scheduled lunar observations have been made at the same phase angle,  $55^{\circ}$  to  $56^{\circ}$  (waning) for Terra MODIS and  $-55^{\circ}$  to  $-56^{\circ}$  (waxing) for Aqua MODIS. In order to meet the phase angle requirement, spacecraft maneuvers (rolls) are often needed. MODIS lunar observations are made through its SV port with data sector rotation operations performed right before and after the lunar observations.

Figure 3 shows examples of Terra MODIS band 1 ( $0.65\mu\text{m}$ ) lunar observations made during a period from September to December 2006. Thus far, more than 95 and 70 lunar calibration events have been scheduled and carried out for Terra and Aqua MODIS, respectively. In addition, both MODIS instruments have acquired many un-scheduled lunar observations. In general, the un-scheduled lunar observations without spacecraft maneuvers have different phase angles. After corrections for the view geometry differences, the un-scheduled lunar observations could also be used for the RSB radiometric stability monitoring and other applications<sup>6</sup>.

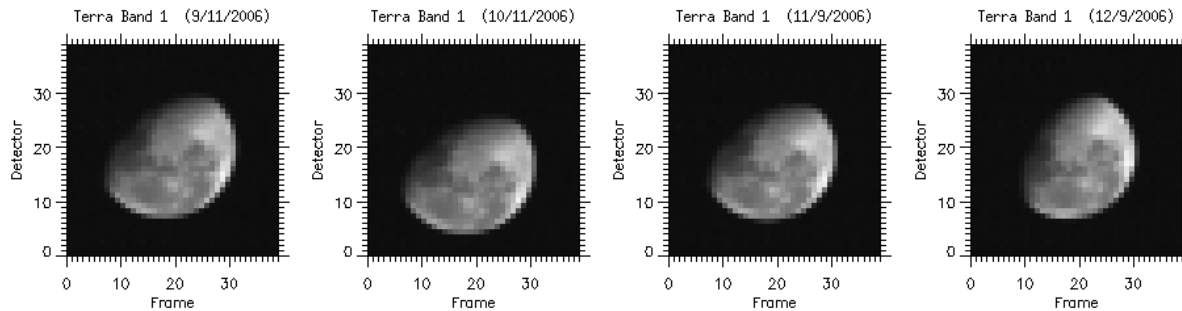


Figure 3: Terra MODIS scheduled lunar observations (band 1 at  $0.65\mu\text{m}$ ) from September to December 2006

## 3. APPLICATIONS OF LUNAR OBSERVATIONS

### 3.1 Lunar Observations for RSB

MODIS RSB on-orbit calibration is performed using its on-board SD/SDSM system. The lunar observations are also made to monitor the RSB radiometric calibration stability. MODIS views the sunlight reflected from the SD and the lunar surface via the same optical system. The only difference is that the SD and lunar observations are made at two different angles of incidence to the scan mirror. Because of this, MODIS lunar observations are used together with SD observations to determine changes in RSB response versus scan angle (RVS)<sup>7-8</sup>. The SD calibration coefficients,  $(m_1)_{SD}$ ,

are derived from detector responses to the SD with corrections for instrument background, temperature, and a number of view geometry-dependent factors. Similarly, lunar calibration coefficients,  $(m_1)_{Moon}$ , require corrections for the lunar view geometry. The RSB calibration coefficients are derived for each band, detector, sub-sample, and mirror side using the following expressions,

$$(m_1)_{SD} = F_{SD} / (dn^*)_{SD}, \tag{1}$$

$$(m_1)_{Moon} = F_{Moon} / (dn^*)_{Moon}. \tag{2}$$

where  $F_{SD}$  is a correction factor, which depends on the SD BRF, thus the SD viewing geometry, its on-orbit degradation, the SD screen transmission if it is in place, and the Earth-Sun distance.  $F_{Moon}$ , is a correction factor that depends on the lunar surface reflectance properties, which are viewing geometry dependent, the Earth-Moon distance, and the Moon-Sun distance.  $(dn^*)_{SD}$  and  $(dn^*)_{Moon}$  are the detector digital responses to the SD and Moon, respectively, with instrument background, viewing angle, and temperature effects corrected. To minimize the effect due to different lunar viewing geometry, lunar observations have been carefully scheduled with the same phase angle for each MODIS instrument.

MODIS has 36 spectral bands and a total of 490 individual detectors. They are located on four focal plane assemblies (FPA) as shown in Figure 4. All MODIS spectral bands are aligned in the cross-track direction and detectors of each band are aligned in the along-track direction. When MODIS views the Moon, the same lunar image gradually moves across all the bands (detectors) on the FPA. The normalized lunar profiles from individual detectors in both directions can be used to derive the detector-to-detector registrations (DDR) and band-to-band registration (BBR). Recently, MCST has developed an approach to use lunar observations to characterize the modulation transfer function (MTF) for the RSB. In addition, MODIS lunar observations have been used for on-orbit characterization of its SWIR detector thermal leak and electronic crosstalk<sup>9</sup>.

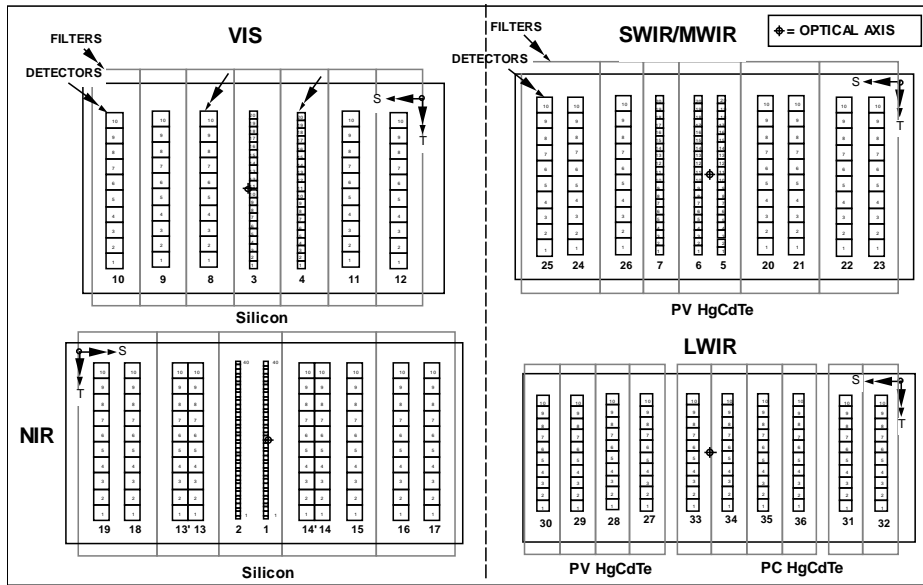


Figure 4: MODIS focal plane assemblies (FPAs): VIS, NIR, SWIR/MWIR, and LWIR.

Another useful application of lunar observations is to enable sensor calibration inter-comparison<sup>10</sup>. This approach can examine calibration differences among sensors and, therefore, help understand and resolve calibration discrepancies between sensors. It can consistently track sensors' radiometric stability even if they are operated on different platforms or over different timeframe. For radiometric stability monitoring and calibration inter-comparison purposes, a lunar radiometric model, such as the one from USGS is needed to provide accurate and consistent corrections for the lunar viewing geometry<sup>11</sup>. Results from MODIS lunar observations show that Terra and Aqua MODIS have been consistently

calibrated to within  $\pm 1\%$  for most RSB. The BBR results derived from MODIS lunar observations generally agree with that derived from its on-board device, a spectroradiometric calibration assembly (SRCA).

### 3.2 Lunar Observations for TEB

With the same philosophy, lunar observations can be applied for the TEB calibration stability monitoring. However, earth-observing sensors normally saturate when viewing the Moon since typical earth scene brightness temperatures are much lower than the Moon. Table 1 is a summary of MODIS TEB key design parameters, including their center wavelengths and bandwidths, typical and maximum specified radiances and temperatures, and noise equivalent radiance and temperature differences. Only band 21, designed for fire detection, has specified maximum temperature above 335K. For Terra MODIS, however, the actual saturation temperatures, also listed in Table 1, are approximately 392, 387, and 374K for bands 31, 32, and 36, respectively.

Table 1: Terra MODIS TEB specifications (CW: center wavelength, BW: bandwidths, L<sub>typ</sub>/L<sub>max</sub>: typical/maximum specified radiances, T<sub>Ltyp</sub>/T<sub>Lmax</sub>: temperature at typical/maximum radiance, NE<sub>dL</sub>/NE<sub>dT</sub>: noise equivalent radiance/temperature difference at typical radiance, T<sub>Sat</sub>: sensor actual saturation temperature)

Band	CW (nm)	BW (nm)	L <sub>typ</sub> (W/m <sup>2</sup> /sr/□)	L <sub>max</sub> (W/m <sup>2</sup> /sr/□)	NE <sub>dT</sub> (K)	NE <sub>dL</sub> (W/m <sup>2</sup> /sr/□)	T <sub>Ltyp</sub> (K)	T <sub>Lmax</sub> (K)	T <sub>Sat</sub> (K)
20	3750	180	0.45	1.71	0.05	0.0010	300	335	335
21	3959	59	2.38	85.44	0.20	0.0154	335	500	478
22	3959	59	0.67	1.89	0.07	0.0019	300	328	329
23	4050	61	0.79	2.16	0.07	0.0022	300	328	330
24	4465	65	0.17	0.34	0.25	0.0022	250	264	317
25	4515	67	0.59	0.88	0.25	0.0062	275	285	316
27	6715	360	1.16	3.21	0.25	0.0108	240	271	323
28	7325	300	2.19	4.47	0.25	0.0172	250	275	319
29	8550	300	9.59	14.55	0.05	0.0090	300	324	330
30	9730	300	3.70	6.34	0.25	0.0219	250	275	358
31	11030	500	9.56	13.26	0.05	0.0070	300	324	392
32	12020	500	8.95	12.10	0.05	0.0061	300	324	387
33	13335	300	4.53	6.56	0.25	0.0183	260	285	334
34	13635	300	3.77	5.03	0.25	0.0161	250	268	341
35	13935	300	3.11	4.42	0.25	0.0141	240	261	341
36	14235	300	2.08	2.96	0.35	0.0154	220	238	374

Since not all the lunar pixels have the same temperatures and the retrieved brightness temperatures vary significantly across the entire lunar surface, only a fixed number of pixels with the highest temperatures are used to track each detector's long-term change caused by its on-orbit calibration. This approach has been applied to Terra MODIS bands 31 and 32. Results from 10 years of lunar observations indicate that Terra MODIS TEB calibration has been generally stable with no obvious drift over its entire mission. For Aqua MODIS, the saturation temperatures are much lower than Terra MODIS and, therefore, this approach cannot be directly applied to Aqua MODIS.

For TEB bands with saturated lunar pixels, we plan to use a fixed number of pixels in the middle temperature range to monitor the changes in detector responses over time. A ratioing approach has been applied to some reflective solar bands that have saturated lunar pixels. A similar approach can also be applied to the TEB in order to characterize their detector-to-detector calibration differences. Since most TEB bands in both Terra and Aqua MODIS saturate when viewing the Moon, the lunar BBR characterization is limited to their VIS and NIR spectral bands.

It was identified from pre-launch that Terra MODIS had experienced an optical leak among TEB photoconductive (PC) detectors (bands 31-36). On-orbit lunar observations have been routinely used to derive the optical leak correction coefficients applied to the LIB algorithm<sup>9</sup>.

## 4. MODIS BAND 21 CALIBRATION

### 4.1 Methodology

Except for band 21 which applies a simple linear algorithm, MODIS TEB calibration uses a quadratic algorithm with reference to the on-board BB on a scan-by-scan basis. As illustrated in Figure 2, band 21 detector responses to the BB and associated SNR are too low to produce useful calibration parameters that can be used to accurately retrieve the high temperature scenes. In this study, an approach is developed as an attempt to apply lunar observations to improve B21 calibration over its entire dynamic range.

For a quadratic algorithm, calibration source radiance (space background and instrument thermal emission subtracted),  $\Delta L_S$ , is related to the corresponding detector responses (background responses subtracted),  $dn_S$ , through a set of quadratic calibration coefficients ( $a_0$ ,  $b_1$ , and,  $a_2$ ),

$$\Delta L_S = a_0 + b_1 dn_S + a_2 (dn_S)^2 \quad (3)$$

Equation 3 can be applied to on-board BB and lunar observation. For TEB on-orbit calibration,  $\Delta L_{BB}$  includes three terms with contributions from the on-board BB, scan mirror, and instrument cavity. For lunar observations,  $\Delta L_{Moon}$  has only two components: one is due to the thermal emission from the Moon and another due to solar reflection from the lunar surface. Thus

$$\Delta L_{Moon} = \varepsilon_{Moon} RVS_{SV} L(T_{Moon}, \lambda) + \text{solar\_reflection}(\lambda) \quad (4)$$

where

$\varepsilon_{Moon}$  is the lunar surface emissivity at wavelength  $\lambda$ ,  
 $RVS_{SV}$  is the response versus scan angle (RVS) at the sensor's space view (SV) angle,  
 $T_{Moon}$  is the temperature of the Moon on a pixel-by-pixel level

In general, the reflected solar contribution is extremely small for the longer wavelength TEB bands, such as band 31. It needs, however, to be considered for the bands at relatively short wavelengths, such as band 21. In order to use Equations 3 and 4 for band 21 calibration, the following steps should be implemented:

1. Apply Equations 3 and 4 to band 31 and compute  $T_{Moon}$  for each pixel
2. Derive lunar emissivity for band 21 wavelength
3. Derive solar reflection for band 21 wavelength
4. Apply Equations 3 and 4 for band 21 calibration

The first step is straight forward as the lunar emissivity at band 31 wavelength can be found from the literature and its solar reflectance term can be ignored<sup>12-14</sup>. To derive the lunar emissivity at the wavelength of band 21, a best fit between band 31 and band 21 spectral radiances from the moon (which depend on lunar emissivity) and to that from the on-board BB is performed. After steps 1 and 2, the solar reflection at band 21 wavelength can be determined at the relatively high end of its detector responses.

### 4.2 Preliminary Results

Figure 5 shows several curves of Terra MODIS band 21 radiances versus band 31 radiances (the right side plot is a zoom-in of the left side) for their detector 5 (production order). In this fitting, 0.9 is used as the lunar emissivity for band 31 and its solar reflection is considered to be negligible. The thick red curve represents data from BB warm-up and cool-down in 2002. The other four curves are constructed with different lunar emissivity and solar reflection values for band 21. In Figure 5, the best lunar emissivity is estimated to be about 0.682. Although the solar reflection is included as a fitting variable, it is still found to be zero after obtaining the best matching of band 21 and band 31 lunar radiances with their BB radiances.

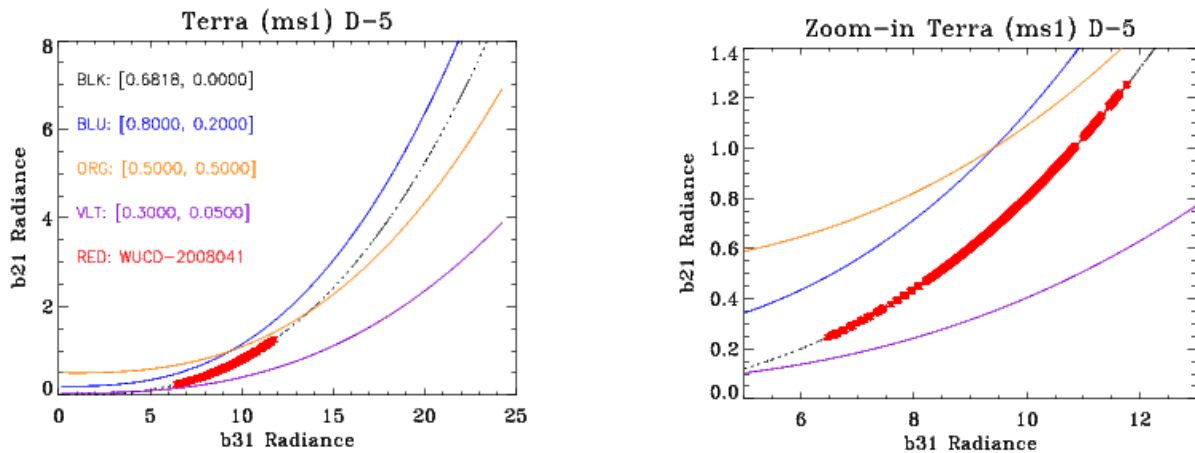


Figure 5: Terra MODIS band 21 and band 31 (mirror side 5 and detector 5) BB and lunar radiances (see text for details). Radiance unit:  $W/m^2/sr/\mu$ .

An alternative approach is to combine steps 2 and 3 and determine the lunar emissivity and solar reflection at the same time by best fitting band 21 lunar data to a curve (line) projected based on band 21 BB calibration data. Two examples are presented in Figure 6 with different lower radiance limits (LR). In this analysis, the emissivity of band 31 is again set to be 0.9. BB WUCD data in 2008 is used. Only detector 5 results are illustrated here. The best emissivity and reflectance estimates are [0.686, 1.169] and [0.674, 1.261] with LR=2 and LR=4, respectively. This study has examined different cases by using different emissivity for band 31 and different lower radiance limits for band 21. Results from 8 out of 10 band 21 detectors (two end detectors excluded) are provided in Figure 7 to help assess the methodology and overall impact due to different input.

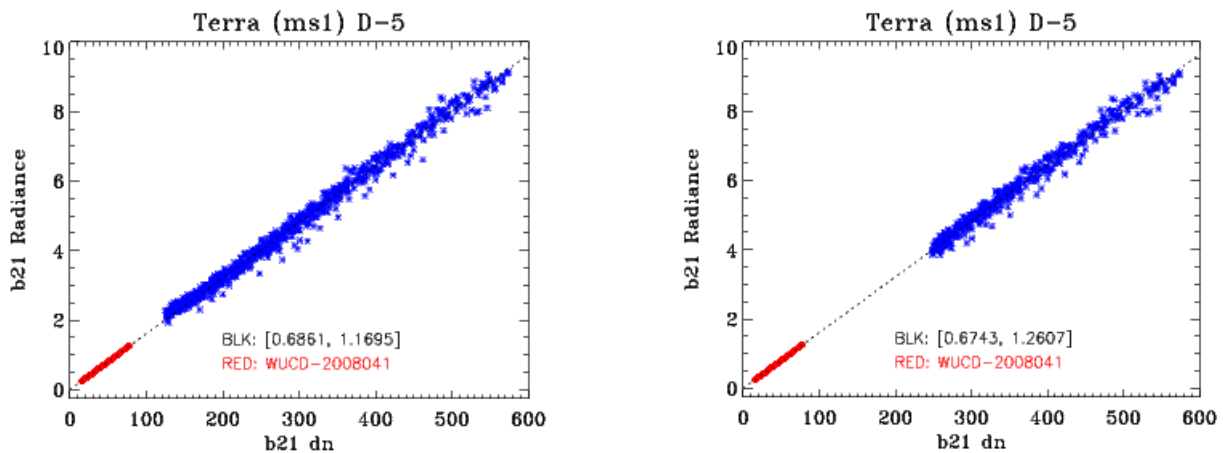


Figure 6: Band 21 lunar emissivity and solar reflection derived with different radiance ranges. Left: lunar data with lower radiances above 2 ( $W/m^2/sr/\mu$ ) are used for best fitting; Right: lunar data with lower radiances above 4 ( $W/m^2/sr/\mu$ ) are used for best fitting.

Some small but noticeable differences among individual detectors are noticed in their retrieved parameters. This is likely due to small differences of individual detectors' view geometry, small time and over-sampling factor differences, and, of course, their calibration differences or uncertainties. With the increase of lower radiance limits, the detector-to-detector differences become much larger. Considering all the features in Figure 7, one could select the best band 21 parameters required for implementing its lunar calibration. With different band 31 emissivity values, the changes in the

band 21 solar reflection term are generally small. On the other hand, the best estimated emissivity is strongly dependent on the knowledge (quality) of band 31 emissivity.

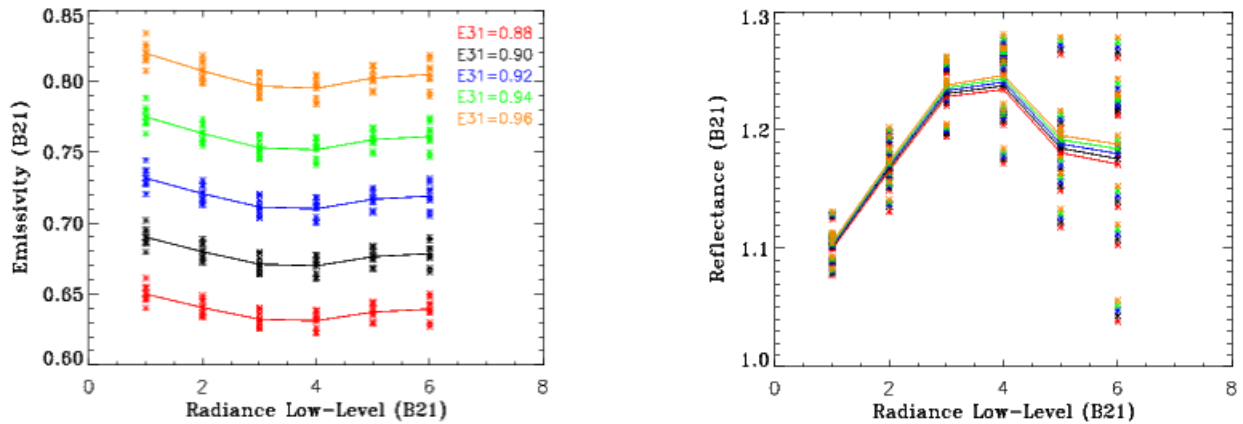


Figure 7: Terra MODIS band 21 (8 middle detectors) lunar emissivity (left) and solar reflection (right) estimations with different band 31 emissivity values and different best fitting lower radiance limits. Reflectance (label) above refers to the solar reflection (Eqn. 4) contribution to the total of lunar radiance of band 21 (in  $W/m^2/sr/\mu$ ).

To improve the band 21 emissivity estimation, we have applied the same approach used in Figure 5 to band 22. This is based on the consideration that band 22 BB calibrations are of higher quality and more stable than band 21 while both bands have nearly the same relative spectral response (RSR). The results from this approach are presented in Figure 8. Again the solar reflection is found to be zero after performing the best matching of band 22 and band 31 lunar radiances to their BB radiances. The best lunar emissivity estimation for band 22 is about 0.681, very close to the band 21 value shown in Figure 5. Another improvement planned for future study is to separate the lunar data with reflected sunlight from those without. For the data without reflected sunlight, we can ignore the solar reflection contribution and focus on the emissivity estimation.

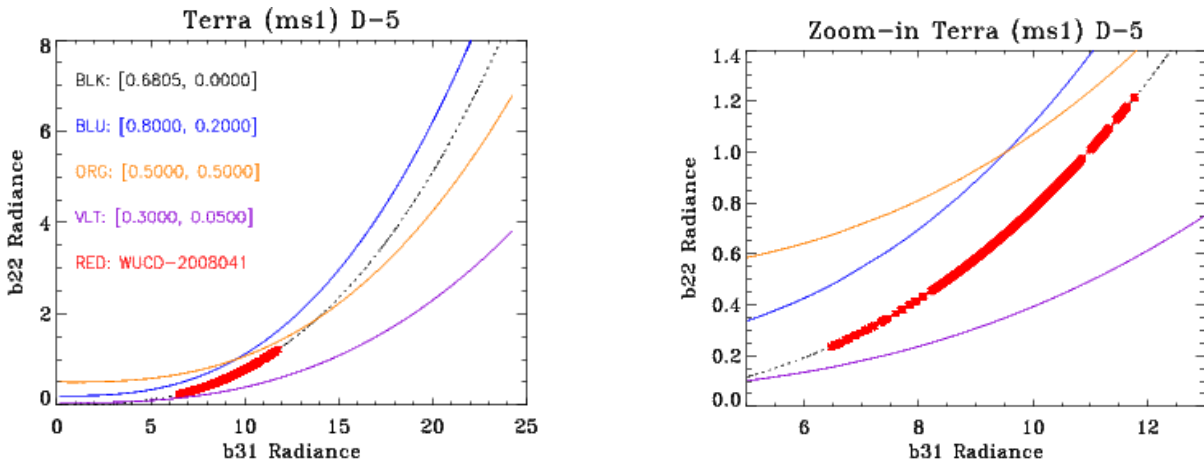


Figure 8: Terra MODIS band 22 and band 31 BB and lunar radiances (see text for details). Radiance unit:  $W/m^2/sr/\mu$ .



## 5. SUMMARY

Lunar observations have been successfully used in support of MODIS on-orbit calibration and characterization for both the reflective solar bands (RSB) and thermal emissive bands (TEB). Applications include using the Moon for sensor radiometric calibration stability monitoring, calibration inter-comparison, band-to-band registrations (BBR) and MTF characterization, and sensor crosstalk (optical and electronic) evaluation. This paper has provided an overview of MODIS lunar observations and their applications developed by the MODIS Characterization Support Team (MCST). It has discussed potential improvements of band 21 on-orbit calibration quality at high temperatures. Different algorithms to estimate band 21 lunar emissivity and solar reflection have been proposed and examined using Terra MODIS lunar observations. Preliminary results indicate that, with additional effort and data analysis improvements, the approaches developed in this paper can lead to good estimates of band 21's lunar emissivity and solar reflection, and thus enable the use of lunar observation to improve band 21 calibration.

## ACKNOWLEDGEMENTS

The authors would like to thank other members of the MODIS Characterization Support Team (MCST), especially T. Chang and G. Toller, for their technical discussions and assistance.

## REFERENCES

1. X. Xiong and W.L. Barnes, "An Overview of MODIS Radiometric Calibration and Characterization" *Advances in Atmospheric Sciences*, 23 (1), 69-79, 2006
2. X. Xiong, K. Chiang, J. Esposito, B. Guenther, and W.L. Barnes, "MODIS On-orbit Calibration and Characterization," *Metrologia* 40, 89-92, 2003
3. J. Sun, X. Xiong, W. Barnes, and B. Guenther, "MODIS Reflective Solar Bands On-orbit Lunar Calibration," *IEEE Transactions on Geoscience and Remote Sensing*, Vol. 45, No. 7, 2383-2393, 2007
4. X. Xiong, K. Chiang, A. Wu, W. Barnes, B. Guenther, and V. Salomonson, "Multiyear On-Orbit Calibration and Performance of Terra MODIS Thermal Emissive Bands", *IEEE Trans. on Geosci. Remote Sens.*, 46(6), pp.1790-1803, June 2008
5. X. Xiong, B. N. Wenny, A. Wu, W. Barnes, and V. Salomonson, "Aqua MODIS Thermal Emissive Bands On-orbit Calibration, Characterization, and Performance," *IEEE Trans. Geosci. Remote Sens.*, 47(3), 803-814, 2009
6. J. Sun, X. Xiong, and W.L. Barnes, "MODIS Reflective Solar Bands Unscheduled Lunar Observations," *Proceedings of SPIE - Earth Observing Systems XII*, Vol. 6677, 66771K, doi: 10.1117/12.732521, 2007
7. X. Xiong, J. Sun, W. Barnes, V. Salomonson, J. Esposito, H. Erives, and B. Guenther, "Multi-year On-orbit Calibration and Performance of Terra MODIS Reflective Solar Bands," *IEEE Transactions on Geoscience and Remote Sensing*, Vol. 45, No. 4, 879-889, 2007
8. X. Xiong, J. Sun, X. Xie, W. Barnes, and V. Salomonson, "On-Orbit Calibration and Performance of Aqua MODIS Reflective Solar Bands," *IEEE Trans. Geosci. Remote Sens.*, 48(1) 535-546, 2010
9. X. Xiong, J. Sun, S. Xiong, and W.L. Barnes, "Using the Moon for MODIS On-orbit Spatial Characterization," *Proceedings of SPIE - Sensors, Systems, and Next Generation of Satellites VII*, 5234, 480-487, 2004
10. X. Xiong, J. Sun and W. Barnes, "Intercomparison of On-Orbit Calibration Consistency between Terra and Aqua MODIS Reflective Solar Bands using the Moon", *IEEE Trans. on Geosci. Remote Sens. letters*, 5(4), pp.778-782, October 2008
11. T. Stone and H. Kieffer, "An absolute irradiance of the Moon for on-orbit calibration", *Proceedings of SPIE - Earth Observing Systems VII*, 4814, 211-221, 2002
12. J. Shaw, "Modeling infrared lunar radiance," *Optical Engineering*, 38(10) pp.1763-1764, 1999
13. J. Salisbury, A. Basu and E. Fischer, "Thermal Infrared Spectra of Lunar Soils," *ICARUS* 130, pp125-139, 1997
14. J. Linsky, "The Moon as a Proposed Radiometric Standard for Microwave and Infrared Observations of Extended Sources," *the Astrophysical Journal Supplement Series*, No.216, pp.163-244, 1973